FLAME INHIBITION BY PHOSPHORUS-CONTAINING COMPOUNDS

FINAL TECHNICAL REPORT

March 1998

E. M. Fisher, F. C. Gouldin, T. M. Jayaweera, M. A. MacDonald
Sibley School of Mechanical and Aerospace Engineering
Upson Hall, Cornell University, Ithaca, NY 14853-7501

DARPA Contract MDA972-97-M-0013

Sponsored by:
The Department of Defense
Strategic Environmental Research and Development Program

TABLE OF CONTENTS

I. SUMMARY

I A. Task Objectives

The objective of this project is to evaluate the effectiveness of phosphorus-containing compounds (PCCs) as alternatives to halons as fire suppressants. PCCs show promise as flame inhibitors but have been little studied in the past. Our objective is to assess the effectiveness of several PCCs as flame suppressants under a variety of flame conditions, using by determining their effect on extinction strain rate in an opposed-jet burner. These measurements provide a basis for deciding whether this class of compounds merits further study as halon alternatives. Another objective is to obtain information about whether the chemical form of the phosphorus plays an important role in flame inhibition.

I B. Technical Problems

The main technical problem in evaluating PCC flame suppression effectiveness was developing a reliable method for performing extinction measurements with low-vapor-pressure additives. A novel method of approaching extinction was developed and validated. This method allows the use of syringe-pump delivery of low-vapor-pressure additives, while avoiding the problem of transient additive loading as flowrates are varied.

I C. General Methodology

The experimental methodology used in this study was the measurement of extinction strain rates in laminar opposed-jet-burner flames. Phosphorus-containing compounds (PCCs) were added to flames, and their effect on the extinction strain rate was determined. The fractional reduction in extinction strain rate was taken as a measure of suppression effectiveness.

Extinction measurements were performed with two PCCs, dimethyl methylphosphonate (DMMP, $P(=O)(-CH_3)(-OCH_3)_2$) and trimethyl phosphate (TMP, $P(=O)(-OCH_3)_3$), as minor flame additives. Several types of flames were investigated with DMMP: pure methane vs. pure air, pure propane vs. pure air, premixed methane/air, and various choices of methane/nitrogen vs.

oxygen/nitrogen. With TMP, only pure methane vs. pure air flames were investigated. Several experiments were performed with inert additives, for comparison. Fuel-side and air-side introduction of the additive were investigated in separate experiments. Maximum additive levels were limited to about 1500 ppm to avoid additive condensation.

In addition to experiments, a literature search on the physical, toxicological and materials compatibility properties of phosphorus-containing compounds was performed. We compiled data about as many PCCs as possible from several reference works.

I D. Technical Results

The PCC additives demonstrated high flame suppression effectiveness under all conditions investigated. When introduced on the air side of pure methane vs. pure air flames, the PCCs showed an effectiveness that was two to four times higher (on a molar basis) than values reported in the literature for CF_3Br, a highly effective halon flame suppressant for which replacements are sought. PCC effectiveness is 40 times higher (on a molar basis) than that of N_2, determined through our own measurements. Effectiveness was linear with loading, and was not strongly influenced by the choice of fuel or by whether the flame was premixed or nonpremixed. The flame suppression properties of PCCs are very unlikely to be due to their hydrocarbon groups, as experiments with isooctane addition to the air side of a methane/air flame produced flame promotion rather than suppression. Under no circumstances was flame promotion by PCCs observed.

Experiments with variable-dilution methane/nitrogen vs. oxygen/nitrogen flames showed, as expected, that the flame location has a strong impact on additive effectiveness. Fuel-side addition became more effective as the stoichiometric mixture fraction increased, and air-side effectiveness showed the opposite trend. When results were normalized by the quantity of additive calculated to be at the flame location, two additional observations were made. (1) Air-side delivery of DMMP to the flame produces significantly higher effectiveness per mole additive at the flame location than fuel-side delivery does. (2) The effectiveness of DMMP has a strong temperature dependence, with lower effectiveness at higher adiabatic flame temperatures. This implies that DMMP flame suppression performance in practical fires, which typically have lower temperatures than those of this study [1], may be even better than that observed here.

A literature search for physical, toxicological, and materials compatibility properties of PCCs was performed, collecting data on 57 compounds. This or similar information can be used to optimize the choice of candidate halon replacements. Most of the compounds listed have low vapor pressure, implying that delivery to the flame in sufficient quantities may require application of the agent in droplet form, either as a pure substance or dissolved in water. PCCs span a wide range of toxicity. Materials compatibility data are sparse, and are not available for several promising compounds. The available information indicates several PCCs are compatible with some metals (stainless steel, Hastelloy, Inconel) and incompatible with others (copper, aluminum, brass). Compatibility with non-metals is fairly good with the exception of Buna-N. More research appears to be needed in this area.

I E. Important Findings and Conclusions

In the current series of experiments, the PCCs TMP and DMMP have shown high flame suppression effectiveness for a variety of nonpremixed flames and for a more limited set of premixed flames. Over the range of conditions tested, effectiveness is linear in loading, and increases as temperature decreases. The extinction results also lead to several tentative conclusions about the mechanism by which PCCs suppress flames. Although the current experiments provide no direct information about the mechanism of action, the high effectiveness of PCCs suggests a chemical mechanism, as opposed to a physical one. Since PCCs' molar effectiveness is even higher than that of CF_3Br, a plausible mechanism might involve catalytic radical recombination pathways in which active suppressant species are recycled. The higher effectiveness (when normalized by the quantity of additive at the flame) of air-side vs. fuel-side delivery of the PCCs also supports this idea, as it suggests that the loading of additive in the region of high radical levels is important. The very similar effectiveness for DMMP and TMP and the flame promotion observed with hydrocarbon additives, are consistent with the hypothesis that phosphorus-containing species formed in the flame, rather than the parent phosphorus-containing compound or its hydrocarbon groups, are key participants in flame suppression reactions.

I F. Significant Hardware Developments

The use of the present burner in extinction measurements with low-vapor-pressure additives is new to this study. This use has required the development of a novel method of approaching extinction. In this method, the flowrate of the doped reactant stream is kept constant, while that of the other stream is increased. As a result, the flame position changes during the approach to extinction. To validate this method, we empirically determined that the extinction strain rate is affected only slightly by flame position over a wide range of positions. Extinction measurements in this acceptable region of the burner were considered valid.

I G. Special Comments

None.

I H. Implications for Further Research

The extremely favorable flame suppression properties of PCCs revealed by this study indicate that this class of compounds merits further research as potential halon replacements. Several types of research would be useful.

First, research is needed on methods of delivering large quantities of relatively low-vapor-pressure PCCs to the flames. For practical applications, it will be necessary to achieve loadings higher than the 1500 ppm achieved here, and considerably higher than the few hundred ppm achievable without preheating of reactants. Options for flame delivery include sprays of solid particulates or droplets of either neat PCCs or PCC/water solutions.

Secondly, it would be useful to test the flame suppression effectiveness of a broader range of PCCs. The current experiment involves two fairly similar PCC molecules. Extending this type of study to other compounds will either strengthen or disprove the hypothesis that the phosphorus content of a molecule is its most important attribute. In the coming year, we plan to build a delivery system for fine droplets that will eventually allow us to test a much broader range of candidate PCCs in our burner.

Thirdly, research into the mechanism of flame suppression by PCCs would be of use in optimizing the choice of PCC for halon replacement. Experiments involving measurements of important chemical species, especially flame radicals and active species containing phosphorus, would be of great use in narrowing the range of possible mechanisms responsible for flame suppression. In the coming year we will be developing capabilities for making measurements of the OH radical, one of the key species believed to be affected by the pres ence of phosphorus.

Finally, it is necessary to investigate materials compatibility, toxicity, and likely global environmental impact of candidate halon replacements. Of these areas, materials compatibility appears to be the one in which the need for more information is most pressing.

II. PAPERS AND ARTIC LES PRESENTED AND SUBMITTED FOR PUBLICATION

II A. Presentations

T. M. Jayaweera, M. A. MacDonald, E. M. Fisher, F. C. Gouldin, "A novel method for evaluationg the effectiveness of low volatility flame inhibitors with an opposed-jet burner," presented at the Fall Technical Meeting of the Eastern States Section, The Combustion Institute, Hartford, CT, October 1997.

M. A. MacDonald, T. M. Jayaweera, E. M. Fisher, F. C. Gouldin, "Inhibition of non-premixed flames with dimethyl methylphosphonate," presented at the Spring Technical Meeting of the Central States Section, The Combustion Institute, Point Clear, AL, April, 1997.

M. A. MacDonald, T. M. Jayaweera, E. M. Fisher, F. C. Gouldin, "Inhibited counterflow nonpremixed flames with variable stoichiometric mixture fraction," presented at the Fall Technical Meeting of the Eastern States Section, The Combustion Institute, Hartford, CT, October 1997.

II B. Submitted Publications

M. A. MacDonald, T. M. Jayaweera, E. M. Fisher, F. C. Gouldin, "Variation of chemically active and inert flame suppression effectiveness with stoichiometric mixture fraction," submitted to the *27th Symposium (International) on Combustion*, The Combustion Institute, December 1997.

M. A. MacDonald, T. M. Jayaweera, E. M. Fisher, F. C. Gouldin, "Inhibition of non-premixed flames by phosphorus-containing compounds," submitted to *Combustion and Flame*, August, 1997.

III. DETAILED PROJECT DESCRIPTION

III A. Experimental Apparatus and Techniques

Experiments were conducted in an opposed-jet burner equipped for use with low-vapor-pressure additives. This burner, which was built for a previous research project, is shown in Fig. 1. The following sections describe the burner, the methods of determining the strain rate, the method of approaching extinction, and the experimental conditions and chemicals used in the experiments.

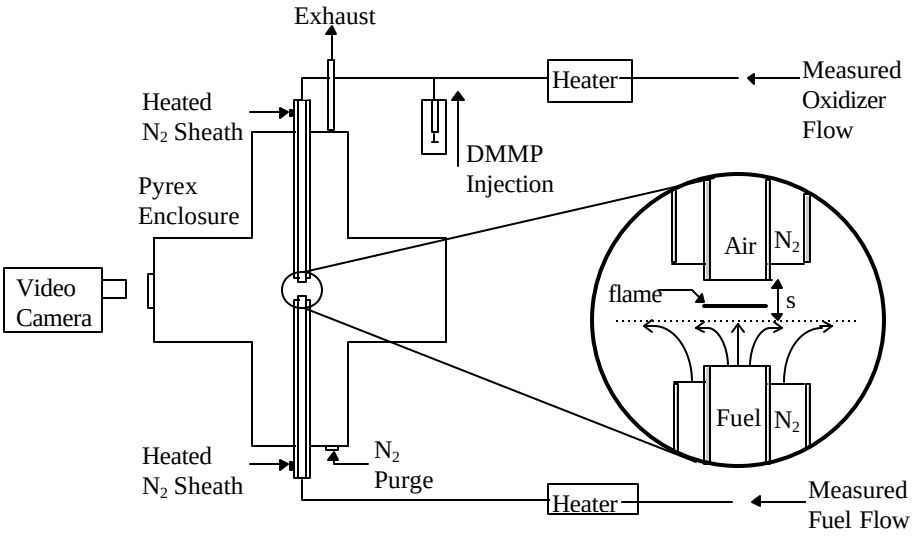

Figure 1. Schematic of the Opposed-Jet burner

III A 1. Burner and Related Equipment

The burner was constructed from straight, open glass tubes 30 cm long with an ID of 0.98 cm, and a separation distance of 0.95 cm between opposing nozzles. No screens or obstructions are used. Annular sheath flows of nitrogen are provided through 2.22-cm ID glass tubes. The sheath tube exits are offset by approximately 1 cm, upstream of the reactant tube exits, to minimize the impact of the sheath flow on the development of the reactant flows. The burner was aligned vertically with the lower tube used as the fuel source and the upper tube as the oxidizer source. Results of a few experiments conducted with the reverse orientation to study the effect of buoyancy showed no significant change in extinction strain rate. A flat flame is produced when the oxidant and fuel stream velocities are such that the flame is situated in the central portion of the space between the burner nozzles. When the flame is close to either nozzle, it exhibits curvature toward the nozzle. The entire burner is isolated in a glass enclosure for control of exhaust gases. This enclosure is purged with nitrogen and maintained slightly below atmospheric pressure. The enclosure has a glass window on one end, approximately 25cm from the centerline of the flow. A video camera, located a few centimeters from this window, was used to measure flame position. Measurements of flame position were

made from magnified images from the camera, displayed on a television screen. Flame position was measured relative to the oxidizer nozzle exit plane using the separation gap between the nozzles for reference.

The PCC additives are liquids at room temperature with low vapor pressures (less than one torr at ambient temperature). In order to maintain sufficient concentrations of the PCC additives in the vapor phase, the reactant lines were heated to approximately 100°C with electrical heating tapes. Wall temperatures on the outside surface of the heated lines were measured with adhesive thermocouples. The temperature of the reactant streams 10 cm upstream from the exit of the nozzles was maintained at 100±1°C via active control of the sheath flow temperature. These final reactant temperatures were measured by sheathed thermocouples in direct contact with the gas flow. The liquid PCC additives was added to the reactant streams via a syringe pump that provides a constant volume flow. The gas flow at the injection site was preheated to approximately 130 °C for a rapid vaporization of the liquid PCC additive. The liquid density, syringe size, and motor speed fixed the mass flow rate of the additive during a given experiment. Previous pyrolysis experiments with DMMP and TMP [2, 3] have shown that thermal decomposition is negligible below 1000 K; thus the preheating of the reactant streams should have no effect on their chemical composition. Mass-flow controllers, supplied by MKS Industries, were used to measure reactant flow rates for the gas-phase reactants: methane, propane, nitrogen, oxygen, and various mixtures of these compounds.

III A 2. Determination of Strain Rates

Strain rates at extinction were determined from fuel and oxidant flowrates, using the following expression:

$$a_q = \frac{2V_O}{L}\left(1 + \frac{V_F\sqrt{\rho_F}}{V_O\sqrt{\rho_O}}\right) \qquad (1)$$

Strain rates determined in this way are referred to as global strain rates.

In Eqn. 1, V_F and V_O respectively represent the average velocities of the fuel and oxidant streams leaving the burner nozzles, as determined from the measured mass flow rates at extinction. ρ_F and ρ_O, the densities of the fuel stream and oxidant, are evaluated at 100 °C. These strain rates

will be referred to as global extinction strain rates. The strain rate expression was derived by Seshadri and Williams [4] for the case of plug flow at the nozzles with an infinitesimally thin reaction zone. Under those conditions, the expression represents the strain rate at the oxidant side of the reaction zone. Although the conditions of our experiments clearly differ from those assumed by Seshadri and Williams, recent work at the Naval Research Laboratory [5] has found a proportional relationship between global strain rates, determined from Eqn. 1, and maximum local velocity gradients upstream of the flame, measured by laser-doppler velocimetry. A proportionality is likely to hold for our burner as well, because of the very similar dimensions and geometry of the burners used in the two studies.

We present extinction data in several forms. For undoped flames, we report the extinction strain rate, a_{qo}, as calculated in Eqn. (1). The subscript o refers to the undoped condition. For flames with an additive, we present the extinction strain rate normalized by the corresponding undoped value (a_q/a_{qo}) or the reduction in strain rate at extinction normalized by the corresponding undoped value ($(a_{qo} - a_q)/a_{qo}$). The latter quantity will be called the effectiveness. In some doped cases, the quantity of additive at the flame location is estimated through a numerical calculation. In these cases, we also report an effectiveness per mole additive calculated to be at the flame, sometimes called the normalized effectiveness.

III A 3. Technique for approaching extinction.

In determining extinction conditions for use in calculating a_q, we made use of a novel method of approaching extinction, motivated by a need to minimize transient effects of additive loading. Commonly, extinction studies with opposed-jet burners adjust the strain rate by varying both the oxidizer and fuel streams simultaneously. With our choice of a constant-mass-flowrate syringe pump for delivering the additive to one of the reactant streams, the conventional procedure results in a change in additive loading during the extinction process. With low-vapor-pressure additives like the PCCs studied here, this changing concentration may produce transients in adsorption or desorption on the tubing and burner walls, and lead to uncertainty in the true loading of additive in the flows at the exit plane of the doped reactant stream at extinction.

The novel method presented here is an alternative technique to circumvent the difficulties associated with additive loading transients. During our experiments, the concentration of

additive in the relevant reactant stream (fuel or oxidizer) was fixed by maintaining constant flowrates of all the constituents of the doped reactant stream. After waiting a sufficient time for equilibrium conditions to be established, we approached extinction by varying only the flowrate of the undoped stream. One consequence of using this method is that the positions of both stagnation plane and flame move towards the doped-stream nozzle during the extinction experiment. This was found to have only a minor influence on the measured extinction strain rate except when the flame or stagnation plane was very close to one of the nozzles, as described below.

We took an empirical approach to validating our novel method of approaching extinction. Experiments were performed over a large range of flow rates of the methane and air streams, achieving extinction with the flame in a variety of positions. Figure 2 shows the resulting global extinction strain rates (a_q) as a function of the measured flame position. In this figure, flame positions inside either nozzle are plotted at the appropriate nozzle location (0 or 9.5 mm from oxidizer nozzle). Extinction strain rate varies systematically with flame position, but the variation is small over a large central portion of the region between the burner nozzles. The global extinction strain rate varies less than (?2% from a mean value of 359 s^{-1} for flame positions between 0 and 7mm. This region of consistent global extinction strain rates will be referred to as the acceptable region. For experiments in which extinction occurs with the flame outside the acceptable region, large deviations in a_q occur. Also shown in Fig. 2 are sets of data from two series of experiments conducted with a 300 ppm doping of DMMP and 50,000 ppm doping of N_2, both in the oxidizer stream. The limited number of data points in the DMMP series is a result of the coarsely quantized mass flow rates of dopant available from the syringe pump. Because of the inhibitory effect of the DMMP or N_2 additive, these data sets have markedly lower mean global extinction strain rates than the data for undoped methane vs. air flames. However, both data sets show the same systematic trends with flame position, and both have only small variations in extinction strain rate over the central acceptable region between 0 and 7 mm.

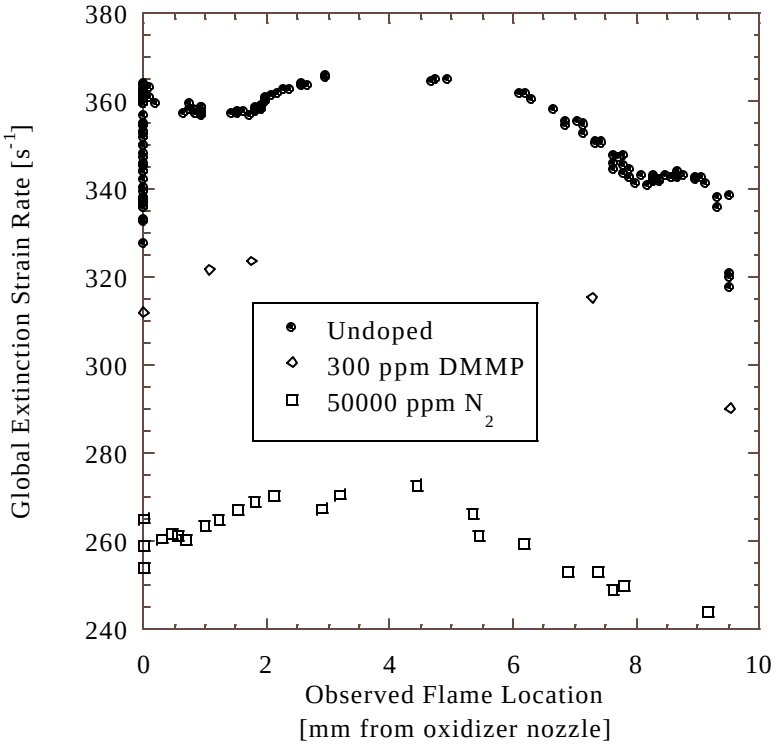

Figure 2. Variation of global extinction strain rate, a_{q}, s^{-1}, with observed flame position at extinction. Methane vs air flames: undoped, doped with DMMP, and doped with N_2. Z_{st}=0.054

A similar acceptable region was found with propane-air non-premixed flames, and is presented in Figure 5 below. In comparison to the methane experiments, these propane flames exhibited considerably more flutter and larger scatter in the observed global extinction strain. However, in the acceptable region, the observed global extinction strain was still found to be within 2.5% of the mean value of 489 s^{-1}.

The existence of the same acceptable region for a range of flame extinction strain rates establishes the validity of our method for approaching extinction. Provided that the flame

position at extinction lies within this region, the results should be consistent to within ?2% (methane/air) or 2.5% (propane/air) of those obtained using more conventional methods that maintain a nearly constant flame position. Caution should be exercised in using this method to measure small changes in strain rate because of the small but systematic variation of flame extinction strain rate with flame position.

The asymmetrical dependence of extinction strain rate on flame position appears to be due to the offsetting of the flame to the oxidant side of the stagnation plane, which is conveniently characterized using the stoichiometric mixture fraction, Z_{st}. (See Section III A 4 for a definition and discussion of Z_{st}.) The importance of this displacement was investigated by performing a series of measurements in which flame and stagnation plane were coincident. Results from these conditions, for methane/nitrogen vs. oxygen/nitrogen flames with $Z_{st} = 0.50$ with $Y_O = 0.387$ and $Y_F = 0.097$, are shown in Fig. 3. During these experiments, in which the oxidizer stream was mixed from separate oxygen and nitrogen source bottles, the global extinction strain rate was very sensitive to the concentration of oxygen. This sensitivity contributed to the greater scatter in the $Z_{st} = 0.50$ tests than in the pure fuel vs. pure air tests, which were conducted with a premixed oxidizer source. Nonetheless, the global extinction strain rate varies less than ?3% of the mean value of 336 s^{-1} for flame locations between 0 and 9mm. Within experimental scatter, results with $Z_{st} = 0.5$ are symmetrical about the center of the region between the two burners.

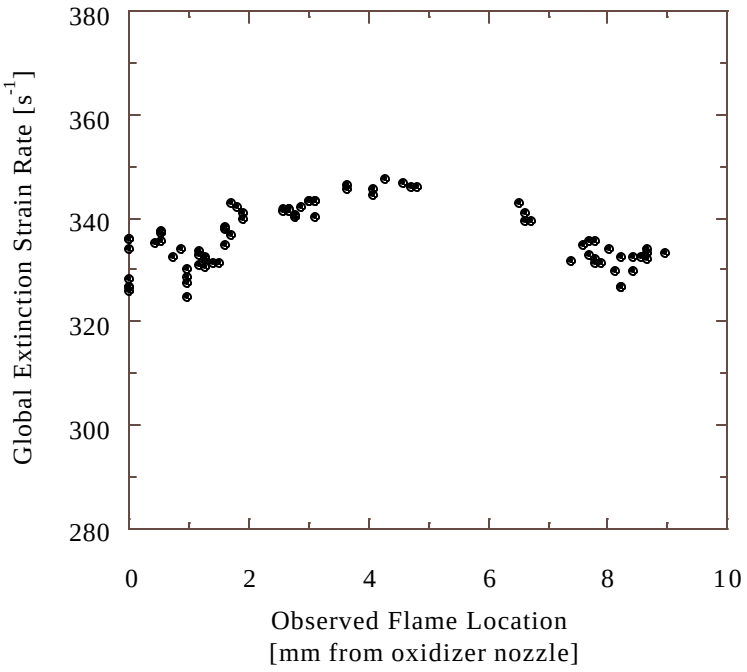

Figure 3. Variation of global extinction strain rate, a_{qo}, s^{-1}, with observed flame position at extinction. Methane/nitrogen vs oxygen/nitrogen flames. Z_{st}=0.5

Although the acceptable region of Figures 2 and 3 is defined in terms of the observed flame position, in practice it is not necessary to determine the experimental observation of flame location at extinction for all measurements. Rather, a parameter S is introduced which can be calculated from the reactant stream properties at the nozzles.

S approximates the distance from the oxidizer nozzle to the stagnation plane and is given by the expression in Eqn. 2, again derived by Seshadri and Williams for plug flow boundary conditions [4]:

$$S = L \Big/ \left(1 + \frac{V_F \sqrt{\rho_F}}{V_O \sqrt{\rho_O}}\right) \qquad (2)$$

Figure 4 shows a plot of observed flame location for both $Z_{st} = 0.50$ and $Z_{st} = 0.054$ against the parameter S. Methane or a methane/nitrogen mixture is the fuel. It is interesting to note that the observed flame location does n ot vary linearly with the predicted location of the stagnation plane, but instead follows a sigmoidal curve, being much more sensitive to flow variations when it is near the middle of the separation gap. The data presented in Fig.4 shows flame positions for only high strain cases (275-360 s^{-1}). It was found that, in general, the steepness of the sigmoidal curve increased with increasing strain rates. For purposes of conducting experiments with the new method, it suffices to observe that the flame locatio n, for each condition, is a well-correlated one-to-one function of this parameter S. Therefore, one can map the experimentally determined acceptable region in terms of S, and direct observation of flame position becomes unnecessary. For both pure methane vs. pure air ($Z_{st} = 0.054$) this region is 3.5 mm < S < 5.25 mm. For methane/nitrogen vs. oxygen/nitrogen with $Z_{st} = 0.5$, the region is 3.5 mm < S < 6.0 mm. For pure propane vs. pure air ($Z_{st} = 0.059$), the region is 3.5 mm < S < 5.25 mm. The extinction strain rate data for the propane vs. air flames are shown as a function of S in Fig. 5 below. All extinction results reported below were for flames inside the more conservative acceptable region obtained for the pure fuel vs. pure air flames.

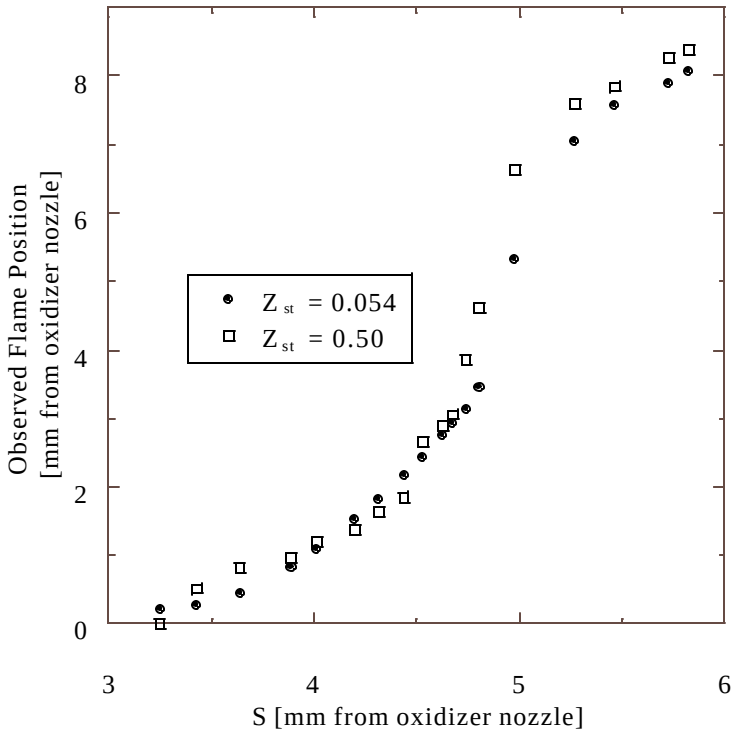

Figure 4. Observed flame positions as a function of predicted distance to the stagnation plane (Eq. 2). Results are shown for nonpremixed methane vs. air flames (Z_{st} =0.054) and methane/nitrogen vs. oxygen/nitrogen flames (Z_{st} =0.5).

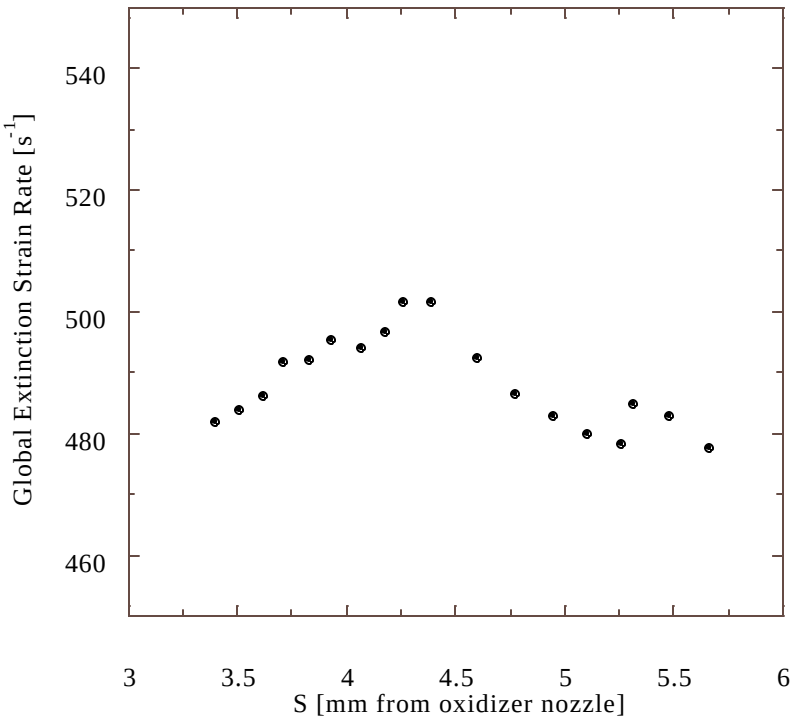

Figure 5. Variation of global extinction strain rate, a_{qo}, s^{-1}, with observed flame position at extinction. Undoped propane vs air flames. Z_{st}=0.059

III A 4. Operating Conditions and Chemicals

We performed several series of extinction experiments. The stoichiometric mixture fraction, Z_{st}, provides a convenient way of characterizing the nonpremixed flames. Z_{st} is the fraction of the material present at the stoichiometric contour that originated in the fuel stream. Z_{st} can be evaluated from reactant compositions in the nozzles and the stoichiometry of the overall combustion reaction, using Eqn. 3

$$Z_{st} = \frac{Y_{o,2}}{\left(\frac{\nu MW_O}{\nu MW_F}\right) Y_{F,2} + Y_{O,2}} \qquad (3)$$

where Y is mass fraction, MW is molecular weight, ν is the stoichiometric coefficient for complete combustion, the subscripts O and F refer to oxygen and fuel respectively, and the subscripts "2" refer to conditions at the fuel and oxidizer nozzles. With the assumption of equal diffusivities for all species, setting $Z_{st} = 0.50$ places the flame at the stagnation plane. Larger and smaller values of Z_{st} correspond respectively to flames on the fuel and oxidant side of the stagnation plane.

Initially, we performed experiments with pure methane vs. pure air and with pure propane vs pure air; these flames, respectively, have $Z_{st} = 0.054$ and 0.059, and correspond to a flame position well on the oxidant side of the stagnation plane. Other experiments were performed with methane/nitrogen vs. oxygen/nitrogen mixtures. In these experiments, Z_{st} was varied systematically. Since the value of Z_{st} depends on two independent variables, Y_F and Y_O, fixing Z_{st} leaves one degree of freedom on reactant concentrations. Except where noted, unique conditions were established by choosing the mass fraction of oxygen to give the same undoped global extinction strain rate as was obtained for the pure methane vs. pure air flame. As Z_{st} is increased with fixed a_{qo}, T_{ad} declines steadily, as seen in Fig. 6.

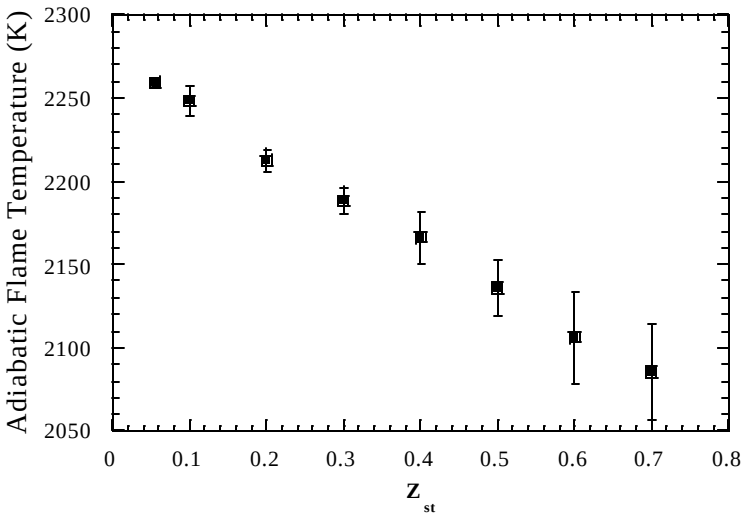

Figure 6.Adiabatic flame temperature as a function of stoichiometric mixture fraction for methane/nitrogen vs. oxygen/nitrogen flames with a_{qp} held constant at 350?10 s^{-1}. Error bars represent standard deviation of data.

A limited number of experiments were performed with twin premixed flames. In these experiments, identical stoichiometric methane/air mixtures flowed from each nozzle.

The PCC additives used during this investigation, dimethyl methylphosphonate (DMMP, $P(=O)(-CH_3)(-OCH_3)_2$) and trimethyl phosphate (TMP, $P(=O)(-OCH_3)_3$), were supplied by Aldrich Chemical Company and used without further purification (stated purity of each compound: 97%). The chemically inert additives nitrogen (99,998% pure) and argon (99.999% pure) supplied by MG Industries. Several series of pure fuel vs. pure air extinction measurements were conducted using premixed oxygen and nitrogen (21?0.2% oxygen mole fraction) or Ultra Zero Grade air (21?2% oxygen mole fraction, total hydrocarbon content <0.1 ppm) as the oxidizer and methane (99% pure) or propane (99.5% pure) as the fuel. All gases were supplied by MG industries. For other extinction experiments, involving premixed flames and variable Z_{st}, oxygen (99.994% pure) was mixed with nitrogen (99.998% pure) in measured proportions to form the oxidizer stream, and the fuel was diluted with nitrogen (99.998% pure).

III B. Extinction Results

III B 1. Undoped Pure Fuel vs. Pure Air Flames and Premixed Flames

Initial tests were conducted with undoped reactant streams at ambient temperature to compare results from our experimental apparatus with those of other researchers. For undiluted methane burning in air, our measured undoped global extinction strain rate was a_{qo} =296 s^{-1}. Variation in a_{qo} up to 80 s^{-1} has been observed with different bottles of high purity compressed air, and is attributed to slightly different batch mass fractions of oxygen. However, extinction measurements on undoped flames using the same oxidizer source are consistent to within ?5 s^{-1}. All results for doped flames presented herein are normalized to undoped experiments under identical conditions, i.e. using the same oxidizer source. This value is comparable to the value found by Puri and Seshadri [6] of 280 s^{-1} and to the value of 255 s^{-1}, computed from flow rates at extinction reported by Papas et al. [7]. All three numbers fall within the range of variation attributed to differences in composition of high purity air batches. This agreement is surprisingly good in light of the significantly different boundary conditions and aspect ratio of the burner used by Puri and Seshadri. Our measured global extinction strain rate differs significantly from literature values of local extinction strain rate, which range from 340 to 400 s^{-1} for experiments [7-9] and from 354 to 544 s^{-1} for numerical calculations [8]. Comparable differences between global and local strain rates are observed by other researchers [7].

For undoped propane vs. air flames, we measured a global extinction strain rate of 489 s^{-1} with reactants at 100 ?C; we did not perform propane extinction measurements with ambient-temperature reactants. Puri and Seshadri [6] report an undoped global extinction strain of 305 s^{-1} with reactant streams at ambient temperature. For methane-air flames, we found that preheating reactants to 100 ?C increased the global extinction strain by 22%. It is expected to have a similar impact on the propane-air flames making a direct comparison of our data with the literature difficult.

For premixed stoichiometric methane/air flames, with reactant streams at 100 ?C, the measured global extinction strain was 873 s^{-1}.

III B 2. Nitrogen in Pure Fuel vs. Pure Air Flames

Further validation experiments were conducted with nitrogen as a chemically inert flame-inhibiting additive. Normalized extinction strain rates for nitrogen addition to the air side of a methane/air flame are shown in Fig. 7.

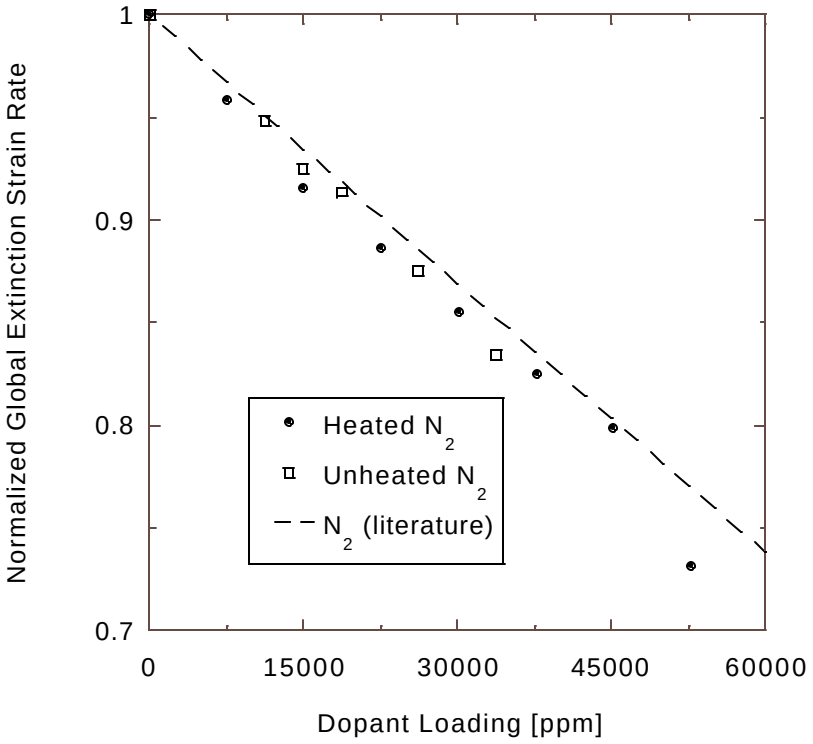

Figure 7. Global extinction strain rate normalized by undoped value (a_q/a_{qo}) for N_2 as an oxidizer-side additive in methane vs. air flames with and without reactant preheating to 100 ?C. Also shown: literature data of Puri and Seshadri [6].

Each data point represents the average of at least three measurements, and is normalized by the extinction strain rate for a pure methane/air flame. Extinction strain rate drops linearly with increasing loading of this additive. Although preheating reactants to 100 ?C has a significant effect on the undoped strain rate (increasing it from 296 to 360 s^{-1}), Fig. 7 shows that it has no

effect on the normalized results. The nitrogen dilution data can be compared to room-temperature data of Puri and Seshadri [6], also shown in Fig. 7. Agreement is good, with least-mean-square slopes agreeing within 7%. However, it should be noted that the diluted flame experiments of Puri and Seshadri were conducted at a fixed value of Z_{st} =0.0544. This requires some nitrogen addition to the fuel-side flow in contrast to our experiments in which nitrogen was added only to the oxidizer stream. Correcting for the effect of this fuel-side addition would lower our measured extinction strain rates by about 3%, resulting in an overall discrepancy of 10% with the Puri and Seshadri data.

III B 3. DMMP and TMP in Pure Fuel vs. Pure Air Flames

Figure 8 shows our results for PCC addition to the air stream of pure methane vs. pure air flames, with reactants preheated to 100 ?C. Each data point represents the average of at least three measurements, and strain rates with additive, a_q, are normalized by the corresponding undoped extinction strain rate, a_{qo}. For DMMP addition, the global extinction strain rate is observed to decrease linearly with additive mole fraction. Experiments indicate that at a mole fraction of 1500 ppm, a_q is reduced by 35% of the undoped value. TMP doping of methane-air flames has a very similar effect on extinction conditions over the common range of loadings. Detectable inhibition (~3% reduction in a_q) is found at loadings as low as 100ppm. For mole fractions below 100ppm, preheating of reactants was not necessary to prevent condensation of DMMP. This allowed for ambient-temperature testing of low DMMP loadings which demonstrated inhibition effectiveness similar to that found in the preheated experiments.

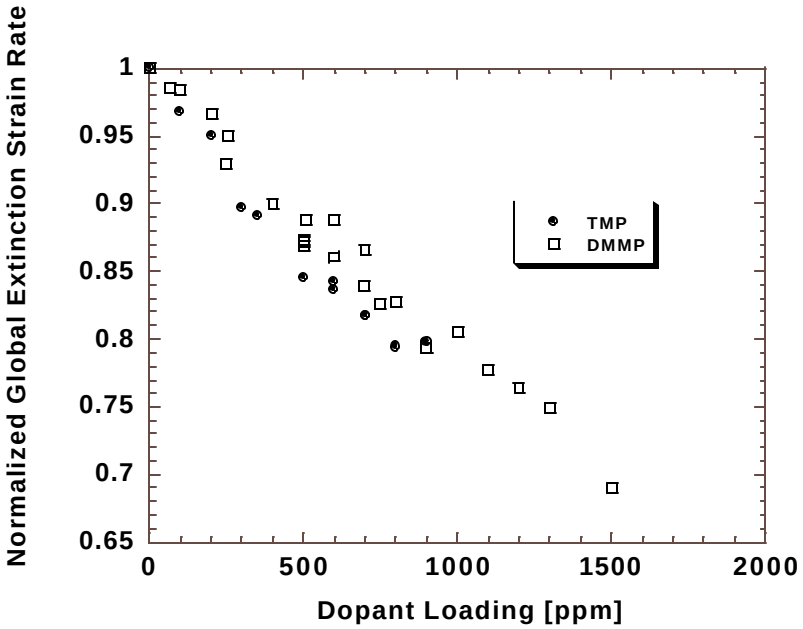

Figure 8. Global extinction strain rate normalized by undoped value (a_q/a_{qo}) for DMMP and TMP as oxidizer-side additives in methane vs. air flames.

Figure 9 shows the normalized global extinction strain rate for DMMP addition to pure propane vs. pure air flames, with data averaging the same as for the methane/air flames above. The greater experimental scatter in these experiments may be associated with the visible fluttering of the higher-strain propane air flames. In an effort to reduce this flutter by lowering the Reynolds number of the reactant flows an additional series of tests was conducted using nozzles with a reduced I.D. of 0.80 cm. The results from these experiments are also shown in Fig. 9. The observed normalized extinction strain rate for DMMP with the smaller nozzles was found to be in reasonable agreement with our standard burner results. Aside from the scatter, both sets of results are very similar to those in pure methane vs. pure air flames.

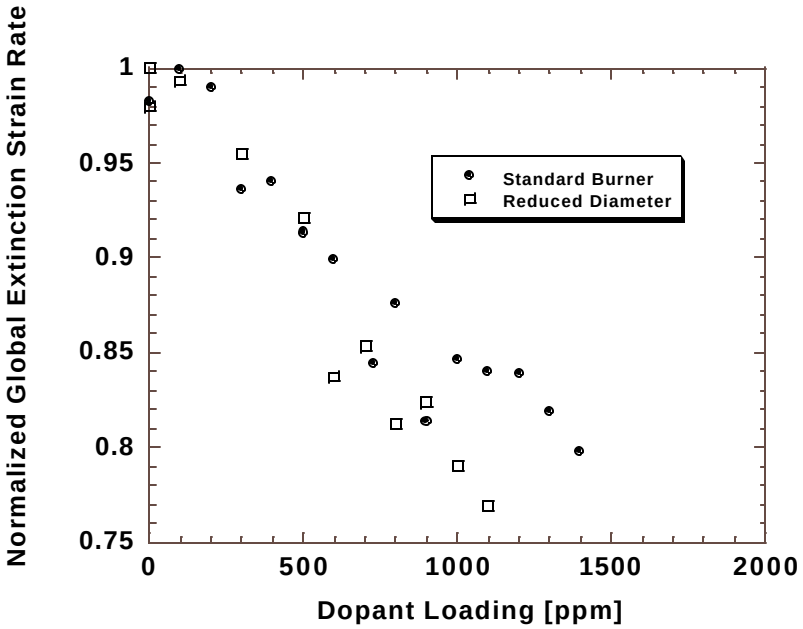

Figure 9. Global extinction strain rate normalized by undoped value (a_q/a_{qo}) for DMMP as an oxidizer-side additive in propane vs. air flames.

III B 4. Isooctane in Pure Fuel vs. Pure Air Flame

We performed an experiment to determine whether the hydrocarbon content of the PCCs contributes significantly to the inhibition effectiveness, perhaps by acting as a radical sink. Tests were conducted with isooctane as the dopant on the air side of a pure methane vs. pure air flame. Isooctane has a similar structure to the PCCs but lacks the central phosphorus atom. It is expected that any contribution from methyl groups to flame inhibition by the PCCs would be observed during the isooctane tests. However, these tests showed a 4% increase in the global extinction strain at a loading of 400 ppm, indicating that the effect of the hydrocarbon was to promote the flame, not to inhibit it. This result provides support for the hypothesis that the phosphorus atom is crucial to the flame inhibition effects of the PCCs studied here.

III B 5. Argon in Methane/Nitrogen vs. Oxygen/Nitrogen Flames

Results from the first series of tests in which Z_{st} varied from 0.2 to 0.7, are shown in Fig. 10. Argon is introduced as an oxidizer-side or fuel-side additive, in a series of flames. In this case we plot the effectiveness, i.e. the reduction in global extinction strain rate normalized by the undoped value, $((a_{qo} - a_q)/a_{qo})$. Each data point represents the average of four extinction measurements. The error bars on the figures represent the standard deviation of the observed values, which in this case is larger than the systematic error due to the method of approaching extinction. As expected, effectiveness with oxidant-side doping decreases as the flame moves towards the fuel side (increasing Z_{st}). The converse is true with fuel-side doping. Argon has a diffusivity similar to that of the reactants; thus, the quantity present at the stoichiometric contour, which determines its effectiveness, should vary roughly linearly with Z_{st}.

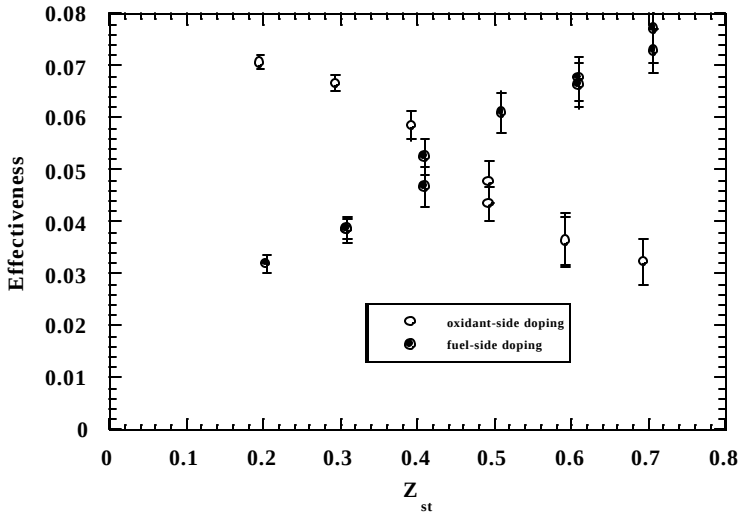

Figure 10. Flame suppression effectiveness of 25,000 ppm argon as an oxidant-side or fuel-side additive in methane/nitrogen vs. oxygen/nitrogen flames with fixed a_{qo}. Effectiveness is defined as $((a_{qo} - a_q)/a_{qo})$. Error bars represent standard deviation of data.

For a quantitative prediction of the amount of additive reaching the flame, we performed detailed numerical calculations of the flame structure, using existing Sandia codes [10-13] with plug flow velocity boundary conditions and multicomponent diffusion but no thermal diffusion. In these calculations, the flame structure was calculated with detailed chemistry, using the GRI

mechanism [14] with nitrogen chemistry omitted. The mole fraction of dopant is evaluated at the maximum temperature contour, taken to represent the flame location.

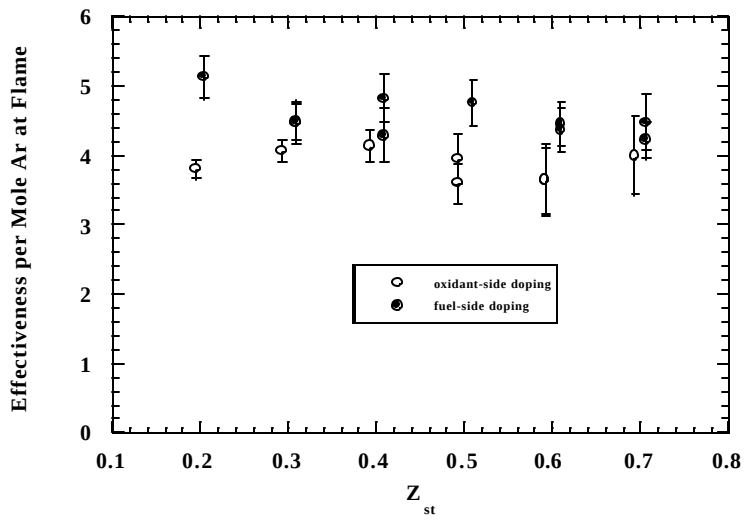

Figure 11. Normalized flame suppression effectiveness for argon in methane/nitrogen vs. oxygen/nitrogen flames with fixed a_{qo}. Effectiveness is normalized by the quantity of argon at the maximum temperature location in the flame, as predicted by a numerical simulation. Error bars represent standard deviation of data and uncertainty in calculated loading.

Figure 11 depicts the argon results, normalized by the numerically predicted quantity of argon present at the maximum temperature contour. These curves of effectiveness per mole at the flame show no trend with Z_{st}, indicating that the concomitant changes in T_{ad} and flame structure, collectively, have no significant influence on the argon effectiveness. Other tests, described below, further demonstrate that the argon effectiveness per mole at the flame is independent of T_{ad}. In addition, Fig. 11 shows no significant difference between oxidizer-side and fuel-side addition for argon flame suppression effectiveness per mole at the flame.

To further clarify the influence of temperature on this system, a series of tests were performed for a fixed $Z_{st} = 0.055$. This experiment was conducted with a fixed composition cylinder of oxygen/nitrogen (21%/79% by volume) and fixed additive flow, greatly reducing

experimental uncertainties. T_{ad} was manipulated by varying the reactant stream temperatures from 22-112 (? 1)°C. This resulted in a range of T_{ad} from 2237-2283 K. There was a significant influence on the overall flame strength, as seen in the variation of a_{qo} from 261-393 s^{-1}. However, the effectiveness for argon at different temperatures varied less than 3% and showed no trend with T_{ad}. These results confirmed that argon's effectiveness has no temperature dependence.

III B 6. DMMP in Methane/Nitrogen vs. Oxygen/Nitrogen Flames

Figure 12 shows the results from extinction measurements performed with DMMP for Z_{st} between 0.055 and 0.7. The observed effectiveness variation with Z_{st} is somewhat more complicated than for the argon tests, although it still follows the same general trend. Each data point in Fig. 12 represents the average of 8 extinction measurements, with error bars representing the standard deviation of the measured values. Differences between individual data points at a given Z_{st} show that tests repeated at identical conditions yielded slightly different results. This variation is attributed largely to the repeatability of the dopant injection system. The dopant effectiveness may also be influenced by small changes in flame temperature resulting from lack of repeatability of the reactant stream compositions. The resulting overall experimental scatter which we observed was significantly higher than the inert tests. The systematic uncertainty due to the method of approaching extinction becomes significant for the oxidizer-side addition tests due to the high observed effectiveness. We estimate an overprediction between 3 and 15% of DMMP effectiveness for this range of conditions due to this systematic uncertainty. The effect is small for the fuel-side addition data.

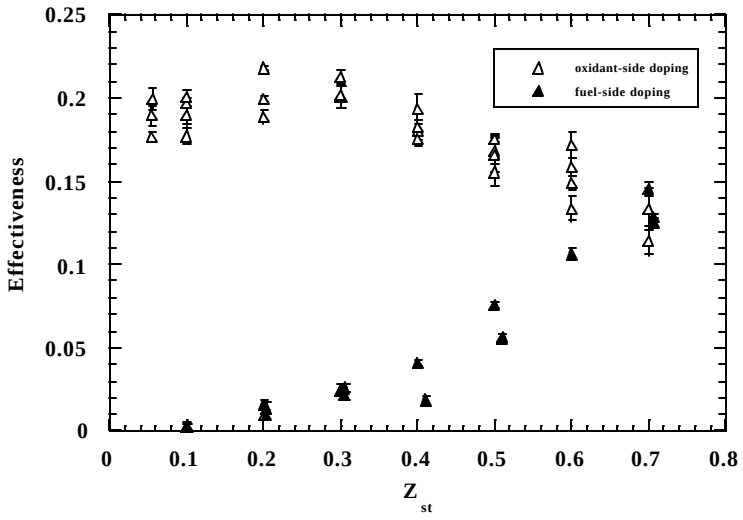

Figure 12. Flame suppression effectiveness of 500 ppm DMMP as an oxidant-side or fuel-side additive in methane/nitrogen vs. oxygen/nitrogen flames with fixed a_{qo}. Effectiveness is defined as $((a_{qo} - a_q)/a_{qo})$. Error bars represent standard deviation of data.

The normalized effectiveness results for DMMP, seen in Fig. 13, have some interesting features. Firstly, it is notable that the DMMP effectiveness per unit mole fraction is roughly 100 times that of argon, indicating strong chemical suppression by DMMP.

Secondly, the curves for oxidizer- and fuel-side addition are offset significantly with respect to one another. The oxidizer-side curve in Fig. 13 displays an effectiveness roughly twice that of the fuel-side curve. The slight systematic overprediction of the oxidizer-side addition effectiveness, described above, would reduce the magnitude of this disparity, but would not reconcile the difference in these curves. The difference between the curves may reflect the importance of the region of high radical levels in the

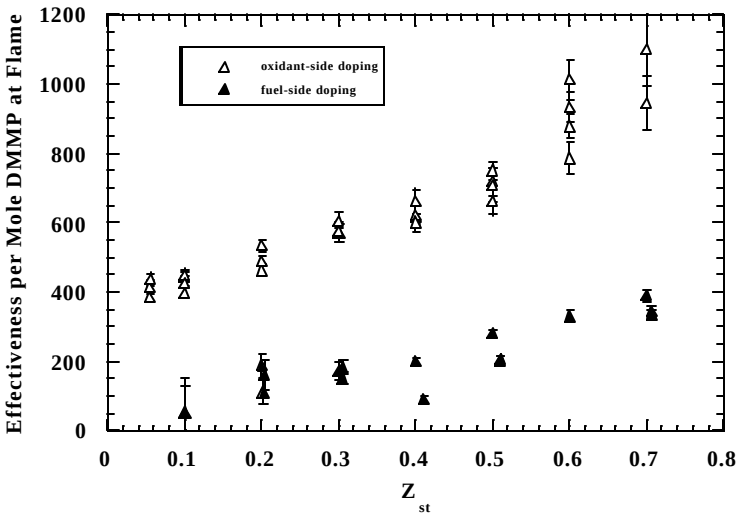

Figure 13. Normalized flame suppression effectiveness for DMMP in methane/nitrogen vs. oxygen/nitrogen flames with fixed a_{qo}. Effectiveness is normalized by the quantity of DMMP at the maximum temperature location in the flame, as predicted by a numerical simulation treating DMMP as inert. Error bars represent standard deviation of data and uncertainty in calculated loading.

suppression process. In most of the flames tested here, key flame radicals are calculated to peak on the oxidant side of the flame. Quantities of additive at the peak radical locations thus would be lower than at the flame location for fuel-side doping, and higher than at the flame location for oxidant-side doping. To test this idea, we performed an alternative normalization of the effectiveness, using the quantity of additive calculated to be at the location at which the reaction $H+O_2$? OH +O has its maximum value. This location is representative of the region of high radical levels. This alternative normalization brings the two curves in Fig. 13 closer together. However, even considering systematic error, oxidant-side doping remains more effective. The disparity between oxidizer- and fuel-side addition may also be associated with the types and quantities of radicals and products that are formed from the parent molecule as it approaches the flame from different directions and their relevance to the suppression action. If we assume that

the important suppression action takes place on the oxidizer side of the flame, then additives to the fuel stream must travel through the flame to reach this point. This may have a significant effect on what phosphorus-containing species are present in the region of important radical chemistry for different modes of addition, i.e. oxidizer- or fuel-side doping.

A final feature of Fig. 13 is that for both the oxidizer- and fuel-side tests, the normalized effectiveness increases with Z_{st}. The existence of this slope implies that the suppressant effectiveness varies with either temperature or structure of the flame, or both. Studies in a variety of premixed flames have indicated that at high temperatures (above 2350 K) [15, 16], DMMP can become a flame promoter. Thus the inhibition effectiveness per mole of DMMP at the flame is expected decrease with increasing flame temperature. Figure 13 is consistent with this expectation, showing decreasing inhibitor effectiveness with increasing adiabatic flame temperature (lower Z_{st} values). However, it is possible that changes in flame structure, which occur at different Z_{st} values, may be influencing suppressant effectiveness as well.

Further tests were conducted to clarify this temperature dependence. Due to condensation of the dopant below 80?C, we were unable to use control of the reactant temperatures to vary T_{ad} over a significant range. Instead, the overall dilution of the flame, at a fixed value of $Z_{st} = 0.5$, was used to vary T_{ad}. In this experiment, the mass fraction of oxygen in the oxidizer stream ranged from 0.39 to 0.44, resulting in a T_{ad} ranging from 2132 to 2261 K and an a_{qo} range of 294 - 572 s^{-1}. Unfortunately, the variation in reactant stream compositions increased the susceptibility of the results to the sensitivity to random uncertainties in relative flowrates, producing considerable scatter. The results from this experiment are shown in Fig. 14, along with the data for oxidizer-side addition at fixed a_{qo}, but varying Z_{st} values; all plotted against T_{ad}. Although the large experimental scatter makes it difficult to draw quantitative conclusions, a clear trend of decreasing effectiveness with increasing T_{ad} is observed, comparable to that seen in the constant a_{qo} data. However, these results do not conclusively eliminate the possibility of flame structure and the detailed chemistry of dopant action influencing dopant effectiveness.

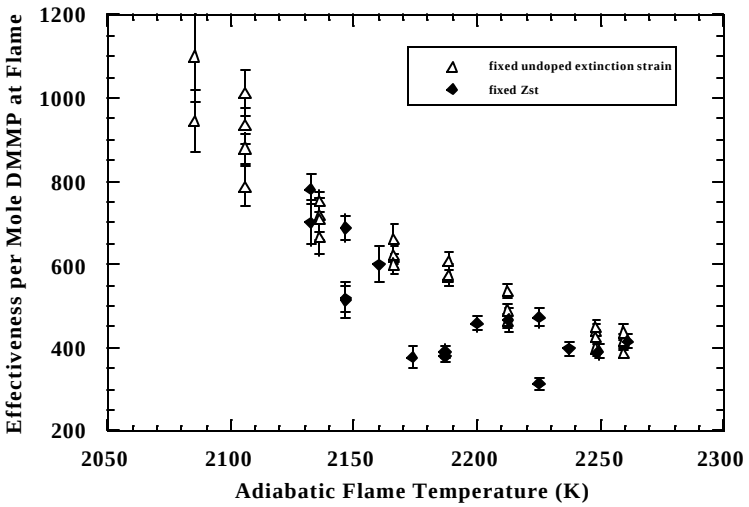

Figure 14. Normalized flame suppression effectiveness for DMMP in methane/nitrogen vs. oxygen/nitrogen flames as a function of adiabatic flame temperature. Triangles represent varying Z_{st} from 0.1-0.7, fixed a_{qo}=350?10 s^{-1}, while diamonds represent fixed Z_{st}=0.5, varying a_{qo} from 294-572 s^{-1}. Effectiveness and error bars as in Fig. 13.

III B 7. DMMP in Premixed Methane/Air Flames

Limited experiments were performed with DMMP addition to one reactant stream in dual premixed stoichiometric methane/air flames. Normalized global extinction strain rate results are shown in Fig. 15. Trends are comparable to those in nonpremixed methane/air flames.

Uncertainties in loading are considerably greater for these experiments than for the nonpremixed ones because of our method of approaching extinction. We chose to dope only one of the premixed reactant streams with DMMP, in order to be able to approach extinction by varying the flowrate of an undoped reactant stream. As in the nonpremixed flames, diffusion across the stagnation plane produces lower loadings at the flame than that in the doped reactant stream. However, in contrast to the nonpremixed flames, the flame position relative to the stagnation plane is strongly affected by the inhibitory properties of the additive. Thus it is impossible to estimate the true loading at the flame without knowledge of the combustion

chemistry effects of the PCCs. The reported loadings can be considered upper bounds on the PCC loading at the flame location for the premixed flames.

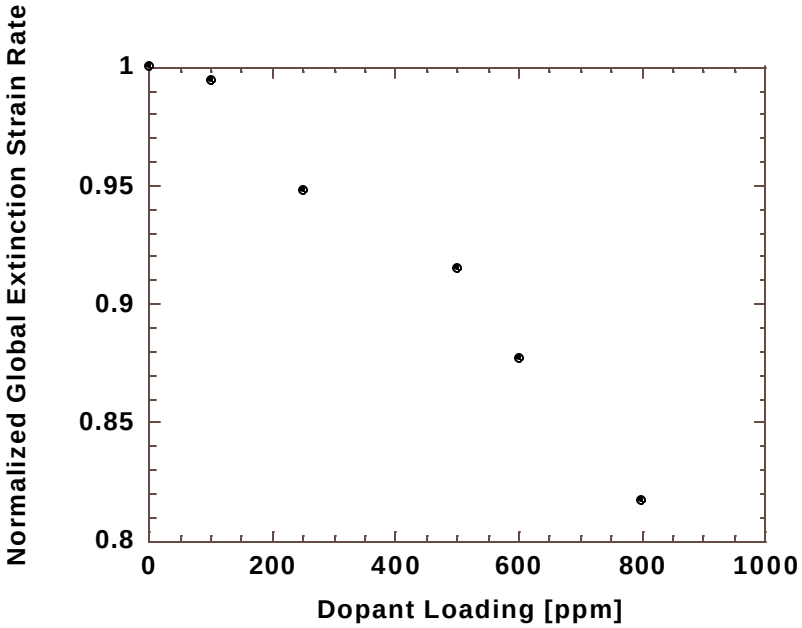

Figure 15. Global extinction strain rate normalized by undoped value (a_q/a_{qo}) for DMMP as an additive in one reactant stream of dual premixed stoichiometric methane/air flames.

III C. Literature Search

A literature search was performed to gather information on relevant properties of PCCs. The results of this survey are given in Appendix A, which lists 57 compounds along with available physical properties, toxicological information, handling requirements, recommended maximum exposure levels, and materials compatibility. If we are correct in believing that the chemical form of the parent compound is not crucial to fire suppression, this or similar information can be used to optimize the choice of candidate halon replacements. Compounds in Appendix A were selected primarily on the basis of availability of information. Several compounds with severe toxicity were deemed unsuitable for fire suppression purposes and

deliberately excluded from the list. An effort was made to include all available information on compounds that have been used in fire-fighting applications or in previous investigations of fire suppression. Data in this table is taken largely from hazardous industrial materials handbooks, manufacturers' listings, and publications of the World Health Organization.

Most of the compounds listed have low vapor pressure, implying that delivery to the flame in sufficient quantities may require application of the agent in droplet form, either as a pure substance or dissolved in water. It is difficult to make generalizations about the toxicity of PCCs. PCCs range in toxicity from non-toxic, essential food constituents and FDA approved additives to some of the most toxic compounds known (chemical warfare agents) [17]. Halogenated PCCs tend to be among the mo re toxic. As a result of the current study, it is clear that halogen atoms are not a requirement for high flame suppression effectiveness. Only limited materials compatibility information was found. This information indicates several PCCs are compatible with some metals (stainless steel, Hastelloy, Inconel) and incompatible with others (copper, aluminum, brass). Compatibility with non-metals was fairly good with the exception of Buna-N. Information was typically unavailable for compounds that were otherwise among the most promising as flame suppressants. It is likely that a more detailed literature review, or an experimental investigation, will be required in order to obtain needed materials compatibility data.

III D. Important Findings and Conclusions

Extinction results for PCC additives are summarized in Fig. 16. These results show very similar flame suppression effectiveness for DMMP and TMP in suppressing methane/air and propane/air nonpremixed flames, and methane/air premixed flames. The similar effectiveness of DMMP and TMP is consistent with the hypothesis that it is phosphorus radicals formed in the flame that are important and not the parent compound. However, it is not a very rigorous test of the hypothesis because DMMP and TMP resemble each other fairly closely.

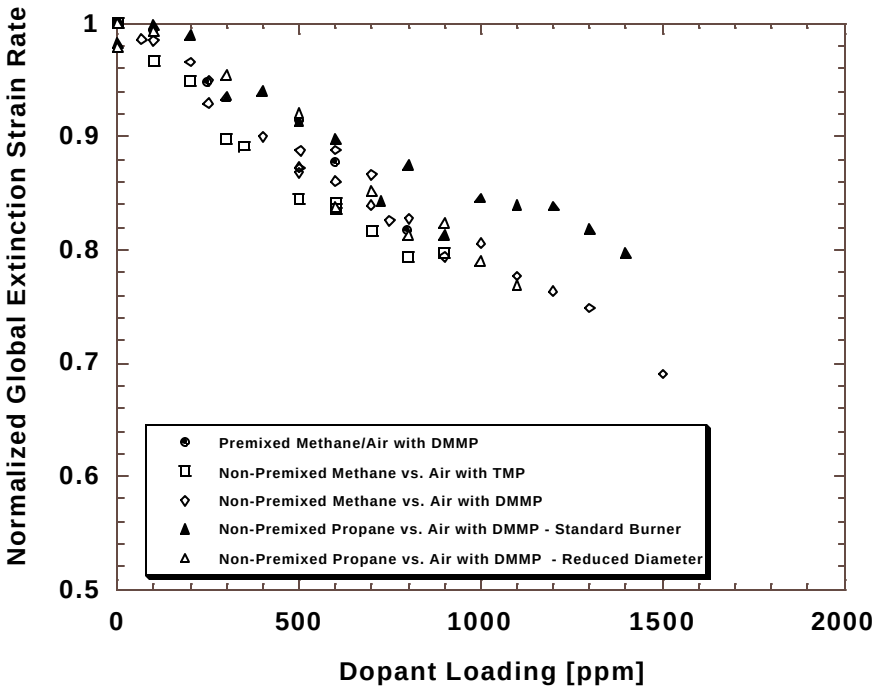

Figure 16. Summary of flame suppression data with PCC additives.

In Fig. 17 we compare flame suppression effectiveness data for DMMP and TMP with literature data [7, 18, 19] for CF_3Br, an effective halon fire suppressant for which replacements are sought. All data sets are for methane vs. air nonpremixed flames, but some of the literature experiments were performed with a Tsuji burner. The flame inhibition properties of DMMP are two to four times better, on a molar or mass basis, than those reported in the literature for CF_3Br. Similar comparisons of DMMP with $Fe(CO)_5$, one of the most effective flame suppressants known, show that $Fe(CO)_5$ is a

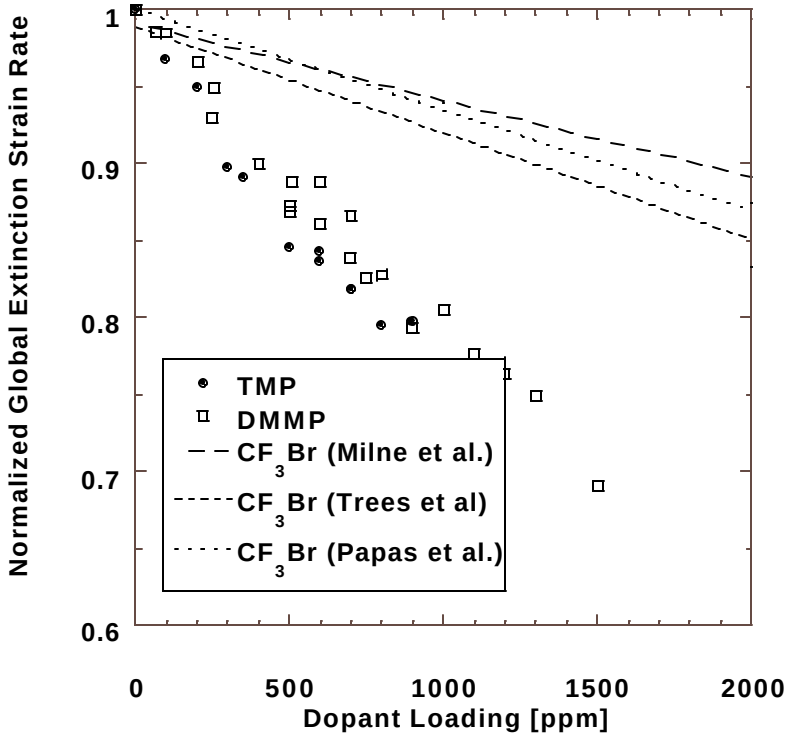

Figure 17. Comparison of DMMP and TMP flame suppression data from the present study with CF_3Br literature data [7, 18, 19]. Methane vs. air flames with air-side addition.

stronger suppressant at low loadings: inhibition at 200 ppm [20] is comparable to the PCC's effectiveness at 1500ppm. However, $Fe(CO)_5$'s effect as an suppressant plateaus for mole fractions between 200 and 500 ppm, the highest gas -phase concentration achievable with ambient temperature reactants [20]. The PCCs' suppression performance can also be compared to the N_2 data presented above: DMMP and TMP are approximately 40 times more effective than N_2 on a molar basis (~10 times as effective on a per mass basis). It is important to note that the range of extinction strain rates achieved in these PCC experiments represents only the upper

portion of the range of local strain rates encountered in a realistic, turbulent, fire [21]. Extending the experimental range to much lower strains would require a different method of introducing the PCC.

Two important observations were made in the experiments in which the dilution of the two reactant streams was varied. (1) DMMP is significantly more effective as a suppressant when added to the oxidizer-side, rather than fuel-side, of the flame, even when results are normalized by the calculated quantity of additive at the flame location. (2) The effectiveness of DMMP has a strong temperature dependence, with lower effectiveness at higher adiabatic flame temperatures. The first observation is consistent with the hypothesis that the PCC acts on the flame radicals, which generally have their highest values on the oxidant side of the flame. The second observation is consistent with previous experiments [16] showing a transition from flame inhibition to flame promotion at high temperatures. Over the conditions of our experiments, no promotion was observed. DMMP's temperature dependence implies that flame suppression performance in practical fires, which typically have lower temperatures than those of this study[1], may be even better than that observed here.

IV. UNRESOLVED TECHNICAL PROBLEMS

Most technical problems related to measuring extinction strain rates in the presence of low-vapor-pressure additives were satisfactorily resolved in the current study. Two unresolved issues remain. First, our justification of the novel method of approaching extinction was entirely empirical. We did not determine the reasons for the existence of a range of flame positions in which dependence of extinction strain rate on flame position is weak. We did not devote time to resolving this issue because we considered the empirical justification of the novel method adequate. Secondly, our method of approaching extinction can not be applied to premixed flames in which both reactant streams are doped. The only alternative that appears to be available for these flames is to approach extinction very slowly, to ensure that adsorption/desorption transients are negligible.

V. RECOMMENDATIONS FOR ADDITIONAL RESEARCH

The extremely favorable flame suppression properties of PCCs revealed by this study indicate that this class of compounds merits further research as potential halon replacements. Several types of research would be useful.

First, research is needed on methods of delivering large quantities of relatively low-vapor-pressure PCCs to the flames. For practical applications, it will be necessary to achieve higher loadings than the 1500 ppm achieved here, and considerably higher loadings than the few hundred ppm achievable without preheating of reactants. Options for flame delivery include sprays of solid particulates or droplets of either neat PCCs or PCC/water solutions. Alternatively, if an acceptable PCC with higher vapor pressure can be found, it may be possible to use current halon delivery systems with fairly minor modifications.

Secondly, it would be useful to test the flame suppression effectiveness of a broader range of PCCs. The current experiment involves two fairly similar molecules. Extending this type of study to other compounds will either strengthen or disprove the hypothesis that the phosphorus content of a molecule is its most important attribute. In the coming year, we plan to build a delivery system for fine droplets that will eventually allow us to test a much broader range of candidate PCCs in our burner.

Thirdly, research into the mechanism of flame suppression by PCCs would be of use in optimizing the choice of PCC for halon replacement. Experiments involving measurements of important chemical species, especially flame radicals and active species containing phosphorus, would be of great use in narrowing the range of possible mechanisms responsible for flame suppression. In the coming year we will be developing capabilities for making measurements of the OH radical, one of the key species believed to be affected by the presence of phosphorus. We plan to use the technique of laser-induced fluorescence to measure this species. For a definitive test of proposed mechanisms, it would also be worth while to develop methods for making quantitative measurements of the important phosphorus-containing radicals in the flame (for example, PO, PO_2, HOPO, and $HOPO_2$). Further work in developing and refining detailed chemical kinetic mechanisms for phosphorus combustion chemistry will also be needed as species measurements become available.

As toxicological and materials compatibility properties will play an important role in determining the viability of PCCs as halon replacements, research in these areas would be of use. At this stage, it may be more fruitful to test the fire suppression effectiveness of compounds with good toxicological and materials properties than to determine the toxicological and materials properties of compounds with good fire suppression effectiveness. Recommendations of compounds or classes of compounds likely to have good toxicological and/or materials compatibility properties are needed. If literature data beyond that covered in our literature search can not be found, a screening study may be in order. Materials compatibility data appear to be especially sparse.

Finally, it is important to consider the potential global environmental impact of PCCs. Although stratospheric chemistry and infrared absorption cross sections for PCCs have not been investigated thoroughly to our knowledge, it is likely that short atmospheric lifetimes of these compounds will guarantee that global environmental impact will be small. Rate constants for several PCCs' reactions with OH have been measured under atmospheric conditions [22-24]. Atmospheric lifetimes estimated from these rate constants range from 3.1 days for TMP to under 3 hours for phosphorothioates. These low values mitigate against any significant effect on the ozone layer or contribution to global warming by PCCs. These conclusions are based on experiments with a limited set of PCCs. If more stable PCCs are under consideration, this subject must be revisited.

VI. CONCLUSIONS

This project assessed phosphorus-containing compounds (PCCs) as alternatives to halons as fire suppressants. The flame suppression effectiveness of two PCCs, dimethyl methylphosphonate and trimethyl phosphate, was evaluated by determining their effect on the global extinction strain rate in opposed-jet flames. For the variety of flames tested, these PCCs showed very high flame suppression effectiveness. Their effectiveness was superior to that of the halon CF_3Br for nonpremixed methane/air flames. For the limited range of PCCs tested, the chemical form of the parent compound appeared to have little effect on flame suppression properties. PCCs show promise as halon replacements. Further research is needed to investigate

their mechanisms of action, to determine important toxicological and materials compatibility properties, and to devise effective ways to deliver them to fires.

VII. REFERENCES

1. Audouin, L., Kolb, G., Torero, J. L., and Most, J. M. *Fire Safety J.* 24:167-187 (1995).
2. Zegers, E. J. P. and Fisher, E. M. *Comb Sci. Tech.* 116-117:69-89 (1996).
3. Zegers, E. J., Flow Reactor Pyrolysis of Alkyl Phosphates and Phosphonates, Ithaca, NY: Cornell University, 1997, pp. 258.
4. Seshadri, K. and Williams, F. *Int. J. Heat Mass Transfer* 21:251-253 (1978).
5. Fisher, E. M., Williams, B.A., Fleming, J.W. *Eastern States Section of the Combustion Institute* (Fall Technical Meeting, Hartford, CT 1997).
6. Puri, I. K. and Seshadri, K. *Combust. Flame* 65:137-150 (1986).
7. Papas, P., Fleming, J. W., and Sheinson, R. S. *26th Symposium (International) on Combustion* 1405-1412 (1997).
8. Chelliah, H. K., Law, C. K., Ueda, T., Smooke, M. D., and Williams, F. A. *23rd (International) Symposium on Combustion* 503-511 (1990).
9. Yang, G. and Kennedy, I. M. *Combust. Flame* 92:187-196 (1993).
10. Lutz, A. E., Kee, R. J., and Grcar, J. F., "OPPDIF: A Fortran Program for Computing Opposed-Flow Diffusion Flames," Sandia National Laboratories, 1994.
11. Kee, R. J., Dixon-Lewis, G., Warnatz, J., Coltrin, M. E., and Miller, J. A., "A Fortran Computer Code Package for the Evaluation of Gas-Phase Multicomponent Transport Properties," Sandia National Laboratories SAND86-8246, 1986.
12. Kee, R. J., Rupley, F. M., and Miller, J. A., "The Chemkin Thermodynamic Data Base," Sandia National Laboratories SAND87-8215B, 1987.
13. Kee, R. J., Rupley, F. M., and Miller, J. A., "Chemkin-II: A Fortran Chemical Kinetics Package for the Analysis of Gas-Phase Chemical Kinetics," Sandia National Laboratories SAND89-8009, 1989.
14. Bowman, C. T., Hanson, R. K., Davidson, D. F., Gardiner Jr., W. C., Lissianski, V., Smith, G. P., Golden, D. M., Frenklach, M., and Goldenberg, M., "GRI-Mech," Ver 2.11, http://www.me.berkeley.edu/gri_mech/.

15. Lask, G. and Wagner, H. G. *8th Symposium (Internatio nal) on Combustion* 432-438 (1960).
16. Hastie, J. W. and Bonnell, D. W., "Molecular Chemistry of Inhibited Combustion Systems," National Bureau of Standards, Final NBSIR 80-2169 ; PB81-170375, 1980.
17. Weil, E. D., "Phosphorus-Based Flame Retardants," in *Handbook of Organophosphorus Chemistry*, Engel, R., Ed. Marcel Dekker, Inc., New York, 1992, pp. 683-738.
18. Milne, T. A., Green, C. L., and Benson, D. K. *Combust. Flame* 15:255-264 (1970).
19. Trees, D., Grudno, A., and Seshadri, K. *Combust. Sci and Tech*. 124:311-330 (1997).
20. Reinelt, D. and Linteris, G. T. *26th Symposium (International) on Combustion* 1421-1428 (1997).
21. Grosshandler, W. L., Gann, R. G., and Pitts, W. M., "Evaluation of Alternative In-Flight Fire Suppressants for Full-Scale Testing in Simulated Aircraft Engine Nacelles and Dry Bays," National Institute of Standards and Technology NIST SP 861, 1994.
22. Atkinson, R., Aschmann, S. M., Goodman, M. A., and Winer, A. M. *Int. J. Chem. Kinet.* 20:273-281 (1988).
23. Atkinson, R., Aschmann, S. M., Arey, J., McElroy, P. A., and Winer, A. M. *Environ. Sci. Technol*. 23:243-244 (1989).
24. Goodman, M. A., Aschmann, S. A., Atkinson, R., and Winer, A. M. *Arch. Environ. Contam. Toxicol*. 17:281-288 (1988).

APPENDIX A. LITERATURE SEARCH RESULTS

Abbreviations and reference numbers are listed after the table.

Compound Name	Chemical formula	CAS #	Sax Rating (1)	Carcinogen (4)
phosphorus (white)	P4	7723-14-0		
phosphorus trioxide	P2O3	1314-24-5	HR 3	
phosphorus pentoxide	P2O5	1314-56-3	HR 3	
phosphine	PH3	7803-51-2	HR 3	
phosphinic acid	O=PH2(OH)	6303-21-5	HR 3	
phosphonic acid	O=P(H)(OH)2	13598-36-2	HR 2	
orthophosphoric acid	O=P(OH)3	7664-38-2	HR 3	
monomethyl phosphonic acid	O=P(H)(OH)(CH3)	13590-71-1	HR 2	
dimethylphosphonate	O=PH(OCH3)2	868-85-9	HR 3	suspected
dimethyl phosphate	O=P(OH)(OCH3)2	813-78-5	HR 1	
trimethyl phosphine	P(CH3)3	594-09-2	HR 3	
trimethylphosphite	P(OCH3)3	121-45-9	HR 2	suspected
dimethyl methylphosphonate	O=P(OCH3)2CH3	756-79-6	HR 2	questionable
trimethyl phosphate	O=P(OCH3)3	512-56-1	HR 3	suspected
trimethyl 2-phosphonoacrylate	(CH3O)2P(O)C(=CH2)CO2CH3	55168-74-6		
Phosphonomycin	O=P(OH)2(CHOCHCH3)	23155-02-4	HR 2	
diethylphosphonate	O=PH(OC2H5)2	762-04-5	HR 2	
triethyl phosphine	P(C2H5)3	554-70-1	HR 3	
triethyl phosphite	P(OC2H5)3	122-52-1	HR 2	
di-(2-ethylhexyl) hydrogen phosphate	O=P(OH)(OCH2CH(C2H5)(C3H8))2	298-07-7		
tris(2-ethylhexyl) phosphate	O=P(OCH2CH(C2H5)(C4H9))3	78-42-2		suspect
triethyl phosphate	O=P(OCH2CH3)3	78-40-0	HR 2	
0-ethylpropyl phosphite	P(OH)2OCH(CH3)(CH2CH2CH3)			
tris (2-ethylhexyl)phosphite	P(OCH2CH(C2H5)(C4H9))3	301-13-3	HR 1	
propyl phosphonic acid	O=P(OH)2((CH2)2CH3)	4672-38-2		
isopropyl phosphonate	O=P(OH)2(OCH(CH3)2)	1623-24-1	HR 2	
diisopropylphosphonate	O=PH(OCH(CH3)2)2	1809-20-7	HR 2	
diisopropyl methylphosphonate	O=P(CH3)(OCH(CH3)2)2	1445-75-6	HR 2	
triisopropylphosphite	O=P[CH(CH3)2]-[OCH(CH3)2]2	116-17-0	HR 3	
tributyl phosphine	P((CH2)3CH3)3	998-40-3	HR 2	
Compound Name	Chemical formula	CAS #	Sax Rating (1)	Carcinogen (4)

tributyl phosphinate	O=P(C4H9)3	814-29-9	HR 3	
dibutylphosphate	O=P(OH)(OC4H9)2	107-66-4	HR 2	
dibutylphosphonate	O=PH(OC4H9)2	1809-19-4	HR 2	
tributyl phosphate	O=P(O(CH2)3CH3)3	126-73-8		
triphenyl phosphine	P(C6H5)3	603-35-0	HR 2	
triphenylphosphite	O=P(C6H5)(OC6H5)2	101-02-0	HR 3	
triphenyl phosphate	O=P(OC6H5)3	115-86-6	HR 3	
tricresyl phosphate aka tritotyl phosphate	O=P(OC6H5CH3)3 (isomer mix)	1330-78-5 78-30-8 563-04-2 78-32-0		no
triisooctylphosphite	O=P(CH2)5CH(CH3)2)(O(CH2)5CH(CH3)2)2	25103-12-3	HR 2	
tris(trimethylsilyl) phosphate	O=P(OSi(CH3)3)3	10497-05-9	HR 2	
diethyl(2-(triethoxysilyl)ethyl)phosphonic acid	O=P(OC2H5)2(CH2CH2Si(OC2H5)3)	757-44-8	HR 1	
ammonium phosphite (salt)	P(OH)2ONH4	51503-61-8	HR 3	
ammonium dihydrogen phosphate	O=P(OH)3 . NH3	7722-76-1	HR 2	
ammonium hydrogenphosphate	O=P(OH)3 . 2NH3	7783-28-0	HR 2	
ammonium metaphosphate				
N-(phosphonomethyl)glycine aka "Glyphosate"	O=P(OH)2CH2(NH)CH2C=O(OH)	1071-83-6	HR 3	
phosphonacetyl-l-aspartic acid	O=P(OH)2(CHC(=O)NHCH(CO2H)CH2(CO2H))	51321-79-0	HR 2	
0,S-dimethyl-N-acetylamido thiophosphate	O=P(CH3O)(CH3S)(NHCOCH3)	30560-19-1	HR 3	
0,0-diethylthiophosphoryl-0-(cyanobenzaldoxime)	S=P(OC2H5)2ON=C(C6H5)CN			
0,0-Di(2-ethylhexyl) dithiophosphoric acid	S=P(SH)(OCH2CH(C2H5)(C4H9))2	5810-88-8	HR 2	
Bromophos	S=P(OC6H2Cl2Br)(OCH3)2	2104-96-3		
phosphorus trichloride	PCl3	7719-12-2	HR 3	
phosphorus oxychloride	O=PCl3	10025-87-3	HR 3	
phosphorus tribromide	PBr3	7789-60-8	HR 3	
2-chloroethyl phosphonic acid	O=PH(OH)2((CH2)2Cl)	16672-87-0		
bis(trifluoromethyl)-chlorophosphine	PCl(CF3)2	650-52-2	HR 3	
tris(2,3-dibromopropyl)phosphate	O=P(OCH2CHBrCH2Br)3	126-72-7		suspected

Compound Name	European Risk and Safety Phrases (4)		RTECS # (4)	Regulated Levels (4)
phosphorus (white)				OSHA 0.1mg/kg
phosphorus trioxide				

phosphorus pentoxide	R35	S22-26	TH3945000	DFG MAK 1mg/m^3
phosphine				EPA 200ppm
phosphinic acid	R34	S26-28-27-36/37/39		
phosphonic acid	R34	S26-28-27-36/37/39		
orthophosphoric acid	R34-22	S26-28-27-36/37/39	TB6300000	OSHA 1mg/m^3
monomethyl phosphonic acid				
dimethylphosphonate	R45-10-20/21/22-36/37/38	S53-16-44-36/37/39	SZ7710000	
dimethyl phosphate				
trimethyl phosphine	R11-36/37/38	S16-26-36/37/39		
trimethylphosphite	R10-34-20/21/22	S16-26-36/37/39-23	TH1400000	OSHA 2ppm
dimethyl methylphosphonate	R20/21/22-36/37/38-40	S23-44-26-36/37/39	SZ9120000	
trimethyl phosphate	R45-46-20/21/22-36/37/38	S53-44-36/37/39-3/7/9	TC8225000	
trimethyl 2-phosphonoacrylate	R36/37/38	S26-37/39		
Phosphonomycin				
diethylphosphonate				
triethyl phosphine	R17-34	S16-27-26-36/37/39		
triethyl phosphite	R10-36/37/38	S16-26-36/37/39-23		
di-(2-ethylhexyl) hydrogen phosphate			TB7875000	
tris(2-ethylhexyl) phosphate			MP0770000	
triethyl phosphate	R22	S25	TC7900000	
0-ethylpropyl phosphite				
tris (2-ethylhexyl)phosphite				
propyl phosphonic acid	R34	S26-28-27-36/37/39	TA0420000	
isopropyl phosphonate				
diisopropylphosphonate	R36/37/38	S26-37/39	SZ7660000	
diisopropyl methylphosphonate				
triisopropylphosphite				
tributyl phosphine	R17-34-20/21/22	S16-26-36/37/39-23	SZ3270000	
Compound Name	European Risk and Safety Phrases (4)		RTECS # (4)	Regulated Levels (4)
tributyl phosphinate	R34-20/21/22		SZ1575000	
dibutylphosphate	R36/37/38	S26-27-36/37/39	TB9605000	OSHA 1 ppm
dibutylphosphonate	R34	S26-27-36/37/39-23	HS6475000	
tributyl phosphate	R22	S25	TC7700000	OSHA 0.2 ppm
triphenyl phosphine	R20/21/22-36/37/38	S26-36	SZ350000	
triphenylphosphite	R22-36/38	S26-36	TH1575000	
triphenyl phosphate	R20/21/22	S36	TC8400000	OSHA 3mg/m^3
tricresyl phosphate	R39/23/24/25	S20/21-28-44	TD0175000	

aka tritotyl phosphate				
triisooctylphosphite				
tris(trimethylsilyl) phosphate	R10-34	S16-26-27-36/37/39	TC9700000	
diethyl(2-(triethoxysilyl)ethyl)phosphonic acid				
ammonium phosphite (salt)				
ammonium dihydrogen phosphate				
ammonium hydrogenphosphate	R36/37/38	S26-36		
ammonium metaphosphate				
N-(phosphonomethyl)glycine aka "Glyphosate"	R20/21/22-36/37/38	S26-36	MC1075000	
phosphonacetyl-l-aspartic acid				
0,S-dimethyl-N-acetylamido thiophosphate				
0,0-diethylthiophosphoryl-0-(cyanobenzaldoxime)				
0,0-Di(2-ethylhexyl) dithiophosphoric acid				
Bromophos				
phosphorus trichloride	R34-37	S7/8-26	TH3675000	OSHA 0.2ppm
phosphorus oxychloride	R34-37	S7/8-26	TH4897000	OSHA 0.1 ppm
phosphorus tribromide	R14-34-37	S26	TH4460000	
2-chloroethyl phosphonic acid	R36/37/38-23/24/25	S26-36	SZ7100000	
bis(trifluoromethyl)-chlorophosphine				
tris(2,3-dibromopropyl)phosphate				

Compound Name	LD50 oral rat mg/kg	Other Toxicology/ Information
phosphorus (white)	3 (4)	
phosphorus trioxide		highly toxic
phosphorus pentoxide	inh rat LC50=1217mg/m^3(1)	
phosphine		Regulatory level is for extreme hazard (1)
phosphinic acid		corrosive, hygroscopic (4)
phosphonic acid		corrosive, hygroscopic (4)
orthophosphoric acid	1530(1)	
monomethyl phosphonic acid	1740(1)	irritant(1)
dimethylphosphonate	3050(3)	
dimethyl phosphate	8714(1)	
trimethyl phosphine		
trimethylphosphite	1600(3)	Severe eye,skin irritant (4)
dimethyl methylphosphonate	8210(4)	
trimethyl phosphate	840(4)	
trimethyl 2-phosphonoacrylate		irritant(4)
Phosphonomycin		intraperitoneal mouse LD50 4000mg/kg(1)
diethylphosphonate	3900(3)	skin-rabbit LD50=2165mg/kg(3)
triethyl phosphine		
triethyl phosphite	3200(1)	
di-(2-ethylhexyl) hydrogen phosphate	4940(4)	corrosive(4)
tris(2-ethylhexyl) phosphate	37000(4)	inhilation gpg LC50=450 mg/m^3(4)
triethyl phosphate	1600(1)	
0-ethylpropyl phosphite	2300(5)	plant growth regulator(5)
tris (2-ethylhexyl)phosphite	10700(1)	slightly toxic(1)
propyl phosphonic acid	3723(5)	plant growth regulator (5), corrosive, hygoscopic (4)
isopropyl phosphonate		corrosive(1)
diisopropylphosphonate	3100(3)	Mildly toxic via skin (3)
diisopropyl methylphosphonate	826(1)	
triisopropylphosphite	167(3)	
tributyl phosphine	750(1)	
Compound Name	LD50 oral rat mg/kg	Other Toxicology/ Information
tributyl phosphinate		

dibutylphosphate	3200(3)	
dibutylphosphonate	3200(3)	severe eye irritant (3)
tributyl phosphate	1400-3000(2)	
triphenyl phosphine	800(1)	inhilation-rat LC50=1135ppm (1)
triphenylphosphite	1600(3)	
triphenyl phosphate	3500-10800(2)	
tricresyl phosphate aka tritotyl phosphate	1160-15800(2)	
triisooctylphosphite	9200(3)	moderately toxic via skin(3)
tris(trimethylsilyl) phosphate	3440(1)	moderately toxic (1)
diethyl(2-(triethoxysilyl)ethyl)phosphonic acid	17200(1)	
ammonium phosphite (salt)		inhilation-rat Lclo=580ppm(1)
ammonium dihydrogen phosphate	5750(1)	
ammonium hydrogenphosphate		low to moderate toxicity (1)
ammonium metaphosphate		
N-(phosphonomethyl)glycine aka "Glyphosate"	470(1), >5000(2), 4873(4)	herbicide (2)
phosphonacetyl-l-aspartic acid		human 862 mg/kg (nonlethal effects)
0,S-dimethyl-N-acetylamido thiophosphate	866-945(5), 700(1)	insecticide (5)
0,0-diethylthiophosphoryl-0-(cyanobenzaldoxime)	2000(5)	insecticide(5)
0,0-Di(2-ethylhexyl) dithiophosphoric acid	4920(1)	skin-rabbit LD50=1250mg/kg(1)
Bromophos	3750-7700(2)	pesticide, 0.4mg/kg human no adverse effect level(2)
phosphorus trichloride	550(1), 18(4)	inhilation rat LC50=104ppm (4 hr) (1)
phosphorus oxychloride	380(1)	
phosphorus tribromide		highly toxic (4)
2-chloroethyl phosphonic acid	4220(5)	plant growth regulator, inh rat LC50=90mg/kg x4hrs (5)
bis(trifluoromethyl)-chlorophosphine		
tris(2,3-dibromopropyl)phosphate	1880-5240(2)	

Compound Name	mp [deg C]	bp [Deg C]/ P [mm Hg]	Vap. Press [mmHg]	Solubility in Water [mg/litre]	Flammability
phosphorus (white)					yes (4)
phosphorus trioxide	24	173(1)			yes (1)
phosphorus pentoxide	340(4)			no (1)	
phosphine	-132(4)	-87(4)		slightly (1)	yes (1)
phosphinic acid				yes (1)	
phosphonic acid					
orthophosphoric acid	41(4)	158(4)	5@25C (4)	yes (1)	no (1)
monomethyl phosphonic acid					
dimethylphosphonate		170(4)			yes (4)
dimethyl phosphate					
trimethyl phosphine	-86(4)	38-39(4)			yes (1)
trimethylphosphite	-78(4)	111(4)		no (4)	yes (4)
dimethyl methylphosphonate		181(4)			yes (1)
trimethyl phosphate	-46(4)	197(4)		yes (1)	
trimethyl 2-phosphonoacrylate		91/0.1(4)			
Phosphonomycin	94(1)			yes(1)	
diethylphosphonate					
triethyl phosphine		128(4)			yes (1)
triethyl phosphite		156(4)			yes (1)
di-(2-ethylhexyl) hydrogen phosphate	-60(4)				
tris(2-ethylhexyl) phosphate		214(4)			
triethyl phosphate	-56(1)	215(4)		yes (1)	yes (1)
0-ethylpropyl phosphite	liquid at ambient temperature (5)			good (5)	
tris (2-ethylhexyl)phosphite					
propyl phosphonic acid	67(4)			good (5)	
isopropyl phosphonate					
diisopropylphosphonate		73/10 (4)			
diisopropyl methylphosphonate					
triisopropylphosphite					
tributyl phosphine		150/50 (4)			
Compound Name	mp [deg C]	bp [Deg C]/ P [mm Hg]	Vap. Press [mmHg]	Solubility in Water [mg/litre]	Flammability
tributyl phosphinate	64-69(4)	150/1.5 (4)			

dibutylphosphate					
dibutylphosphonate		118/11 (4)			
tributyl phosphate	-80(2)	150/10 (2)	9Pa@25C (2)	1012(4C), 2.85*10^-4(50C) (2)	no (2)
triphenyl phosphine	79(4)	377(4)		no (1)	yes (1)
triphenylphosphite	23(4)	360, 150/0.1 (4)		no (4)	yes (4)
triphenyl phosphate	49-50(4)	245/11 (4)		0.7-2.1 (2)	yes(1), no (2)
tricresyl phosphate aka tritotyl phosphate	-33 (2)	241-255/4 (2)		0.35mg/litre (2)	no (2)
triisooctylphosphite					
tris(trimethylsilyl) phosphate	3(4)	228/720 (4)			yes (1)
diethyl(2-(triethoxysilyl)ethyl)phosphonic acid					
ammonium phosphite (salt)					
ammonium dihydrogen phosphate	190(4)			yes (1)	
ammonium hydrogenphosphate	155(1)			yes (1)	
ammonium metaphosphate					
N-(phosphonomethyl)glycine aka "Glyphosate"	185(4)			10100 (2)	no (1)
phosphonacetyl-l-aspartic acid					
0,S-dimethyl-N-acetylamido thiophosphate	80(1)			satisfactory (5)	
0,0-diethylthiophosphoryl-0-(cyanobenzaldoxime)	3(5)	102/0.01(5)		7mg/litre(5)	
0,0-Di(2-ethylhexyl) dithiophosphoric acid					
Bromophos					
phosphorus trichloride	-118(1)	76(1)		no (1)	yes (1)
phosphorus oxychloride	1(4)	105(4)			
phosphorus tribromide	-40(1)	175(1)			
2-chloroethyl phosphonic acid	66(4)			good (5)	
bis(trifluoromethyl)-chlorophosphine					yes(3)
tris(2,3-dibromopropyl)phosphate	5.5(2)	390(2)		no(2)	no(2)

Compound Name	Metal Compatibility [mils of penetration per year] (6)		
	<2	<50	>50 (incompatable)
phosphorus (white)	br (T<15), hast BCD, SS, nb, ni	al, st, Cu	br (T>20)
phosphorus trioxide			
phosphorus pentoxide		al, SS, hast BD	hast C, Cu, st
phosphine			
phosphinic acid			
phosphonic acid			
orthophosphoric acid	hast B D(T<60)C, SS 304	hast BDG, SS, inc	al, br, nb, st, Cu, ni
monomethyl phosphonic acid			
dimethylphosphonate			
dimethyl phosphate			
trimethyl phosphine			
trimethylphosphite			
dimethyl methylphosphonate			
trimethyl phosphate			
trimethyl 2-phosphonoacrylate			
Phosphonomycin			
diethylphosphonate			
triethyl phosphine			
triethyl phosphite			
di-(2-ethylhexyl) hydrogen phosphate			
tris(2-ethylhexyl) phosphate			
triethyl phosphate			
0-ethylpropyl phosphite			
tris (2-ethylhexyl)phosphite			
propyl phosphonic acid			
isopropyl phosphonate			
diisopropylphosphonate			
diisopropyl methylphosphonate			
triisopropylphosphite			
tributyl phosphine			
Compound Name	Metal Compatibility [mils of penetration per year] (6)		
	<2	<50	>50 (incompatable)

tributyl phosphinate			
dibutylphosphate			
dibutylphosphonate			
tributyl phosphate		al, SS, st, hast BC, ni	
triphenyl phosphine			
triphenylphosphite			
triphenyl phosphate			
tricresyl phosphate aka tritotyl phosphate			
triisooctylphosphite			
tris(trimethylsilyl) phosphate			
diethyl(2-(triethoxysilyl)ethyl)phosphonic acid			
ammonium phosphite (salt)			
ammonium dihydrogen phosphate			
ammonium hydrogenphosphate	hast B, SS 304,400	nb, hast C, inc, SS 316	al, br, st
ammonium metaphosphate		al, st, hast, inc, ni, SS	Cu, br
N-(phosphonomethyl)glycine aka "Glyphosate"			
phosphonacetyl-l-aspartic acid			
0,S-dimethyl-N-acetylamido thiophosphate			
0,0-diethylthiophosphoryl-0-(cyanobenzaldoxime)			
0,0-Di(2-ethylhexyl) dithiophosphoric acid			
Bromophos			
phosphorus trichloride	st	hast C, inc, ni	al, Cu
phosphorus oxychloride		al, hast BC, inc, ni	st, br
phosphorus tribromide			
2-chloroethyl phosphonic acid			
bis(trifluoromethyl)-chlorophosphine			
tris(2,3-dibromopropyl)phosphate			

Index Key for Toxicology and Materials Compatibility Data on Phosphorus-Containing Compounds

Sources:

(1) Sax, N. I., and Lewis, R. J., "Dangerous Properties of Industrial Materials", 7th ed., Van Nostrand Reinhold, New Yo rk, 1989.

(2) World Health Organization, "Organophosphorus Insecticides: A General Introduction", Environmental Health Criteria, Vol 63, Finland, 1986.

World Health Organization, "Phosphine and Selected Metal Phosphides", Environmental Health Criteria, Vol 73, Finland, 1988.

World Health Organization, "Tricresyl Phosphate", Environmental Health Criteria, Vol 110, Finland, 1990.

World Health Organization, "Triphenyl Phosphate", Environmental Health Criteria, Vol 111, Finland, 1991.

Mensink, H., Janssen, P., World Health Organization, "Glyphosate", Environmental Health Criteria, Vol 159, Finland, 1994.

van Esch, G. J., World Health Organization, "Tris (2,3-dibromopropyl) phosphate and Bis(2,3-dibromopropyl) phosphate", Environmental Health Criteria, Vol 173, Finland, 1988.

(3) Kaizerman, J. A., Tapscott, R. E., "Advanced Streaming Agent Development, Volume III: Phosphorus Compounds", NMERI 96/5/32540, 1996

(4) Lenga, R.E., Votoupal, K. L. eds, "The Sigma-Aldrich Library of Regulatory and Safety Data", Milwaukee, WI, 1992.

(5) Mel'nikov, N. N., "Organic Compounds of Phosphorus", Joint Publications Research Service, Arlington, VA, 1975.

(6) Schweitzer, P.A., "Corrosion Resistance Tables", 3rd ed, rev. and expanded, Dekker, New York, 1991.

European Risk and Safety Phrases (Ref. 4 above)	
Code	Phrase
R10	Flammable
R11	Highly flammable
R14	Reacts violently with water
R17	Spontaneously flammable in air
R20/21/22	Harmful by inhalation, in contact with skin and if swallowed
R22	Harmful if swallowed
R23/24/25	Toxic by inhalation, in contact with skin and if swallowed
R34	Causes burns
R35	Causes severe burns
R36/37/38	Irritating to eyes, respiratory system and skin
R36/38	Irritating to eyes and skin
R37	Irritating to respiratory system
R39/23/24/25	Toxic: danger of very serious irreversible effects through inhalation, in contact with skin and if swallowed
R40	Possible risks of irreversible effects
R45	May cause cancer
R46	May cause heritable genetic damage
S3/7/9	Keep container tightly closed in a cool, well ventilated place
S7/8	Keep container tightly closed and dry
S16	Keep away from sources of ignition - No smoking
S20/21	When using do not eat, drink or smoke
S22	Do not breathe dust
S23	Do not breathe vapour
S25	Avoid contact with eyes
S26	In case of contact with eyes, rinse immediately plenty of water and seek medical advice
S27	Take off immediately all contaminated clothing
S28	After contact with skin, wash immediately with plenty of water

S36	Wear suitable protective clothing
S36/37/39	Wear suitable protective clothing, gloves and eye/face protection
S37/39	Wear suitable gloves and eye/face protection
S44	If you feel unwell, seek medical advice (show the label where possible)
S53	Avoid exposure - obtain special instructions before use

Abbreviations used in Materials Compatibility Listings

Metals:

ss-Stainless Steel

br-Brass

al-Aluminum

hast-Hastelloy

ni-Nickel

cu-Copper

st-Carbon Steel

nb-Naval Bronze

inc-Inconel

Nonmetals:

tfn-Teflon

pvc-Polyvinyl Chloride

rub-Natural Rubber

pyr-Pyrex

kal-Kalrez

bn-Buna-N

v-Viton

c-Carbon

epx-Epoxy

si-Silicon Rubber